SAND2015-1438J

# THE HISTORY AND EVOLUTION OF OPTICALLY ACCESSIBLE RESEARCH ENGINES

**Paul C. Miles**
Sandia National Laboratories
Livermore, CA, USA

## ABSTRACT

The development and application of optically accessible engines to further our understanding of in-cylinder combustion processes is reviewed, spanning early efforts in simplified engines to the more recent development of high-pressure, high-speed engines that retain the geometric complexities of modern production engines. Limitations of these engines with respect to the reproduction of realistic metal test engine characteristics and performance are identified, as well as methods that have been used to overcome these limitations. Lastly, the role of the work performed in these engines on clarifying the fundamental physical processes governing the combustion process and on laying the foundation for predictive engine simulation is summarized.

## INTRODUCTION

From the very beginning of the development of the internal combustion engine, visualization of the in-cylinder mixing process and the ensuing combustion process has been essential for furthering our understanding of the operation of these devices and for obtaining insight into how their efficiency and emissions can be improved. Visualization studies today still serve this purpose – after over a century of application, studies in optically accessible engines continue to provide new, and sometimes startling, information. Many times what is obvious once it has been observed had not yet even been imagined to take place. Moreover, even for phenomena that may have been guessed at, or even stated, we should bear in mind the words of W.T. Lyn: "One should not under-estimate the value of confirmation, even of an accepted idea."

With the advent of computer simulation as an engine design and optimization tool, optical studies have taken on an additional role: provision of quantitative data regarding the flow and scalar (temperature, composition, etc.) fields in engines over as wide a spatial extent and over as broad a crank-angle range as possible. These quantitative studies serve two inter-related purposes: first, to provide the data necessary to devise computationally tractable models of the in-cylinder processes governing combustion and emissions; and second, to validate and develop confidence in the accuracy of these tools.

In this review of the history of optically accessible engines, the focus is primarily on the unique characteristics of the engines themselves, and how these characteristics evolved to enable measurements of the desired quantities. In the process, it will be impossible to ignore concurrent advances in the optical measurement techniques applied to these engines, though a description of these techniques is not a main objective. Optical studies in related devices, particularly rapid compression machines and constant-volume combustion chambers ('bombs') have also been invaluable in advancing our understanding and in providing quantitative data for model development and validation. However, due to space constraints, we restrict our attention here to engines that are capable of continuous operation, whether fired or motored. Likewise, there is no intent to diminish the important contributions that have come out of engines instrumented (sometimes extensively!) with fiber optics or with the minimal modifications need to employ visualization through an endoscope. Such engines have been particularly invaluable for understanding the behavior and diagnosing problems with serial production engines; however, they are outside the scope of this history. Engines equipped with spark plugs or glow plugs modified to permit temperature, velocity, and/or fuel-air ratio measurements also fall into the category of important devices that cannot be covered here.

Lastly, it would be negligent not to mention the role played by other non-optical measurement techniques including ion probes, thermocouples, hot-wires, fast-acting sampling valves, exhaust gas analyzers, and the ubiquitous cylinder pressure transducer. Careful analysis of the data provided from these devices often relegates optical measurements to playing the

aforementioned role of confirmation. A highly recommended, broader review of reciprocating engine diagnostics has been provided by Amman [1], to which the reader is enthusiastically referred.

## EARLY PRE-WW2 WORK

### Spark ignition (SI) engines

Perhaps the earliest example of the use of an optical engine to better understand the flow and mixing phenomena in reciprocating engines was provided by Nicolaus Otto himself in 1872. Figure 1 shows his hand-cranked model engine employing a glass cylinder. Hand-rolled cigarettes to provide smoke for visualization studies are clearly visible affixed to the engine head on the left-hand side of the photo. Despite his efforts, Otto was said to be so convinced that his engine operated with a stratified charge that it cost him his patent protection in several countries [1]. The existence of a vigorous in-cylinder mixing process, likely to destroy any mixture stratification, was expressed in 1885 by Clerk [2]. Clerk described his prior work using glass models of the Otto engine as demonstrating that "the mixture becomes practically homogeneous even before compression commences."

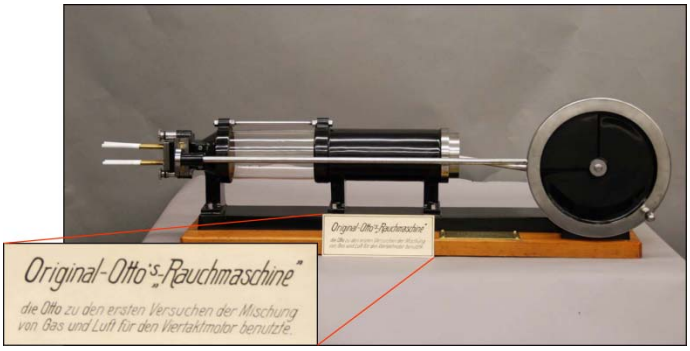


Figure 1. Nicolaus Otto's original "smoke machine". Photo courtesy of Bengt Johansson and Mattias Richter, Lund University.

During the early days of SI engine development, developing an understanding of the laws governing the progress of combustion and subsequent development of the cylinder pressure was a major objective of engine research. A second major objective was development of an understanding of engine knock, which was (and remains) the single most formidable obstacle to the development of high compression ratio engines. Later, having gained significant insight into the processes governing the progress of combustion, and having recognized the importance of the flow field – and turbulence in particular – on the rate of heat release, engine researchers moved their focus to obtaining a better understanding of engine flows.

Late in the 1920's, Sir Harry Ricardo and co-workers [3, 4] reported on the use of an optically accessible side-valve engine to measure the speed of flame travel within the combustion

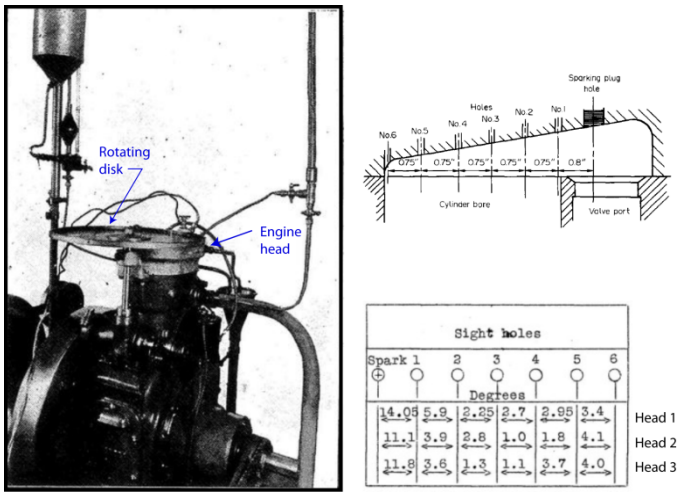


Figure 2. Ricardo's optically accessible head equipped with a rotating disk 'stroboscope', and an example of flame arrival data obtained with three different heads. Figure adapted from Refs [3,4]

chamber. In this engine (Figure 2) a removable head was fitted with a row of 6 windows placed at equal intervals from the spark plug. The windows were sequentially masked by a large rotating 'stroboscopic' disk driven by the camshaft, and by varying the phasing of the disk the crank angle at which the flame arrived beneath each window could be observed visually. Cylinder pressure was also measured, providing a simultaneous record of the movement of the flame and the corresponding pressure rise. One of the significant findings from this work was the observation that even 'heavy' knock generally occurs after the flame has traveled most of the way across the cylinder. Ricardo further concluded that the shape of the combustion chamber and a central spark location were critical factors impacting the maximum usable compression ratio.

Marvin and Best [5] later extended Ricardo's 1927 work, outfitting a similar side-valve engine with 31 windows and employing a rotating disk set-up much like Ricardo's to allow the flame arrival at each window to be determined. Sodium bicarbonate was added to the charge to increase flame luminosity, in an early example of the development and enhancement of an optical diagnostic technique. Like Ricardo, Marvin and Best investigated various spark locations, but also examined the impact of variables such as fuel-air ratio, spark timing, engine speed, fuel type, and compression pressure on the observed 'inflammation' times. They identified the slower combustion of rich and lean mixtures, the near independence of flame speeds on cylinder pressure, and the impact of residual gases on slowing flame speeds. Although Clerk was clearly aware in 1885 that flame speeds increased 'automatically' with engine speed, Marvin and Best provided a direct measurement of this phenomenon. They further noted a direct proportionality of flame speed to engine speed and a 10-fold increase over flame speeds measured in a geometrically similar quiescent chamber. With remarkable prescience, they hypothesized that "increasing the engine speed greatly increases the raggedness of

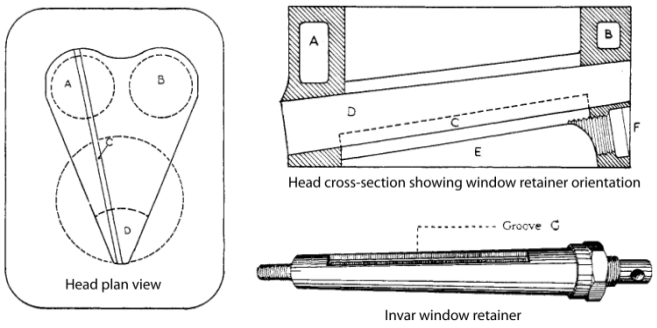


Figure 3. Withrow & Boyd's [6] rectangular window (groove C) spanning the combustion chamber and the Invar® window retainer

the flame front, and consequently its effective area, which permits it to ignite a given volume of charge in a much shorter time." This principle forms the basis of many models of turbulent combustion in use today.

During the same time period, researchers at General Motors Research Laboratories [6] outfitted an engine with a rectangular quartz window that traversed the length of their combustion chamber (Figure 3). To minimize stresses on the window caused by differential thermal expansion, the window was mounted in a special Invar® retainer. This engine was used with a specially developed camera that allowed the propagation of the flame to be captured as a function of time. For normal combustion, the flame kernel was observed to initially grow slowly before the flame reached a roughly steady propagation velocity; under incipient knocking conditions, auto-ignition was observed in the end-gas after the flame had traversed approximately 80% of the combustion chamber. For conditions of heavy-knock the location of auto-ignition was not readily resolved, but it was observed that the remaining volume of unburned charge burst nearly simultaneously into a highly luminous flame. Several possible modes of inflammation of the end gas was thought to be consistent with their results: single or multiple ignition points within the end gas, near simultaneous ignition of the entire volume, or a rapid increase in the propagation speed of the normal combustion zone to near infinity.

To shed light on the chemistry of engine knock, this engine was also fitted with a stroboscopic disk similar to that used by Ricardo, and employed with a spectrograph to examine how the spectral characteristics of the flame emissions varied when knocking combustion occurred and how fuel composition and anti-knock additives affected these emissions [7]. The observation of natural chemiluminescent emissions, visible through windows in the head, was soon supplemented by absorption measurements performed in either the end-gas region or in normal combustion regions closer to the flame [8, 9]. These measurements required a further innovation in optically accessible engines – the incorporation of opposed, rectangular windows in the block (Figure 4a). Measurements obtained in this engine linked the appearance of formaldehyde in the end-gas to knock, and demonstrated that knock

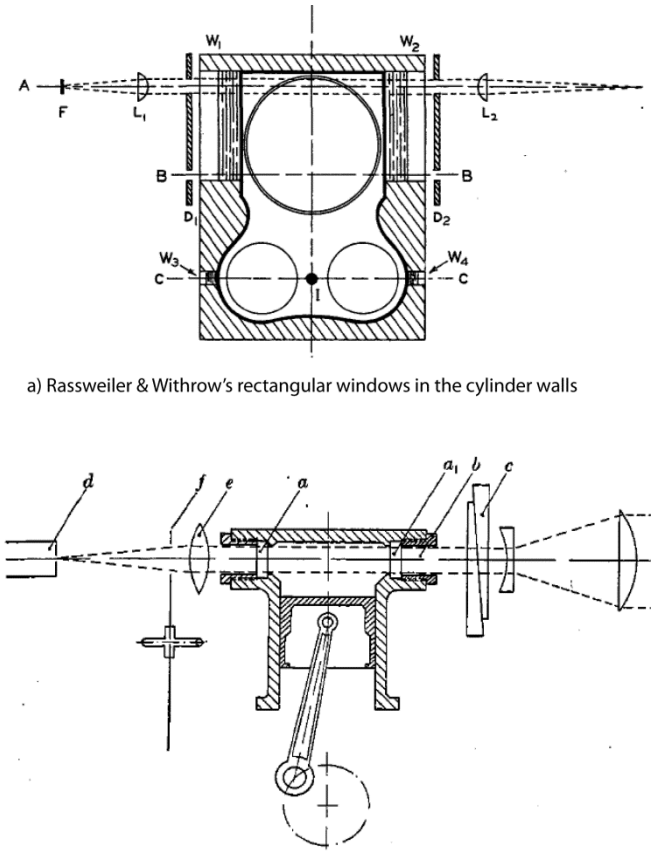


Figure 4. Early examples of placing optical windows in the cylinder walls

suppression by tetraethyl lead appeared to rely on a different mechanism than did knock suppression through the addition of aniline.

Optical access through the rectangular windows in the block was also used to obtain temperature measurements via the sodium line reversal technique, and showed that at the end of combustion there was a significant temperature gradient in the cylinder, wherein the gases closest to the spark plug were over 300°C higher than the last charge to burn. This has a significant impact on $NO_x$ formation, and while the existence of such temperature inhomogeneities had long been suspected (see, for example, Clerk [2]), this was its first measurement in an operating reciprocating engine. Similar measurements, in an engine with more limited optical access through the block, were also reported by Watts and Lloyd-Evans in 1934 [10] and by Hershey and Paton [11]. Notice that the engine used by Watts and Lloyd-Evans, shown in Figure 4b, recessed the windows into the cylinder wall, an early example of potentially compromising the engine geometry to enable optical access. The Hershey and Paton design, in contrast, had its windows mounted flush with the cylinder walls, but the need to use an aviation gasoline to prevent carbon deposits from forming on the windows was reported.

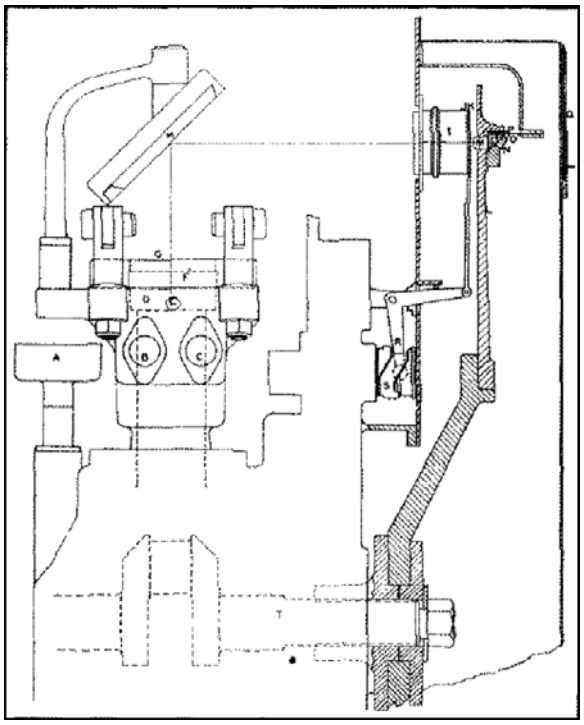

Figure 5. Schematic of Rassweiler and Withrow's engine with full access to the combustion chamber, and the optical arrangement for obtaining high-speed motion pictures

In 1936 Rassweiler and Withrow significantly improved the optical access into the combustion chamber of the General Motors Research Laboratories engine through use of a quartz plate that allowed a complete view of the combustion chamber [12]. As will be discussed below, similar optically-accessible side-valve engines continued to be used by engine researchers for the next 40+ years. Like the earlier rectangular window, the quartz plate was cemented into an Invar® frame. To take advantage of this increased optical access, Rassweiler and Withrow also developed a custom-made drum camera allowing a sequence of photographs to be obtained every 2.4°CA, corresponding to 5000 frames per second at an engine speed of 2000 rpm (Figure 5). Perhaps the most notable outcome of the work performed on this engine was the establishment that the mass of charge burned, as indicated by the combustion images, could be deduced from the measured cylinder pressure and volume histories [13]. This seminal work laid the foundations for the quantitative analysis of the combustion process from measurement of the cylinder pressure.

The inevitable extension from a limited number of windows in the block to the incorporation of a fully transparent cylinder shortly followed the pioneering work of Withrow and Rassweiler [8, 9], Watts and Lloyd-Evans [10], and Hershey and Paton [11]. Motivated by the desire to better understand how air motion assisted the fuel-air mixing process in direct-injection engines, researchers with the National Advisory Committee for Aeronautics (NACA) reported on a study of airflow in a motored engine equipped with a 12.7 mm thick

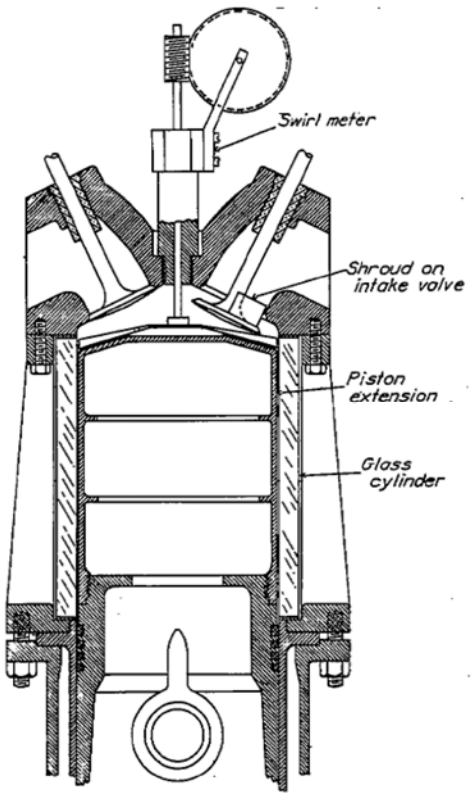


Figure 6. NACA's 1939 optically-accessible engine equipped with a full quartz liner [14]

glass liner supported by a steel casting , shown in Figure 6 [14]. The combustion chamber geometry was remarkably close to that of a modern, pent-roof SI engine equipped with four-valves. Notice the hollow piston extension that was required in order to accommodate the glass liner, which was placed between the engine block and the head. The piston extension did not incorporate sealing rings, but rather kept a sidewall clearance of just 0.4 mm. Nevertheless, the effective 'ring-land crevice' was very large, a problem that still plagues optical engines.

By either shrouding the valves or modifying the port geometry with modeling clay, various degrees of flow swirl could be induced in the cylinder. Air flow studies and flow-spray interaction studies were conducted using chopped goose down as flow tracer particles at speeds up to 1000 rpm. (Speed was limited by blurring of the motion pictures obtained, not the engine). The displacement of individual feathers in a direction perpendicular to the camera axis was also measured to provide a quantitative measure of gas velocity, and the scatter in the gas velocity measurements at a fixed crank angle was taken to be a measure of flow turbulence. Without valve shrouds, the air motion in the cylinder was predominantly chaotic, although some organized tumble motion was detected. In general, however, shroud orientations that produced the greatest amount of flow swirl were observed to produce the least 'turbulence' (the most reproducible flow), and the amount of flow swirl

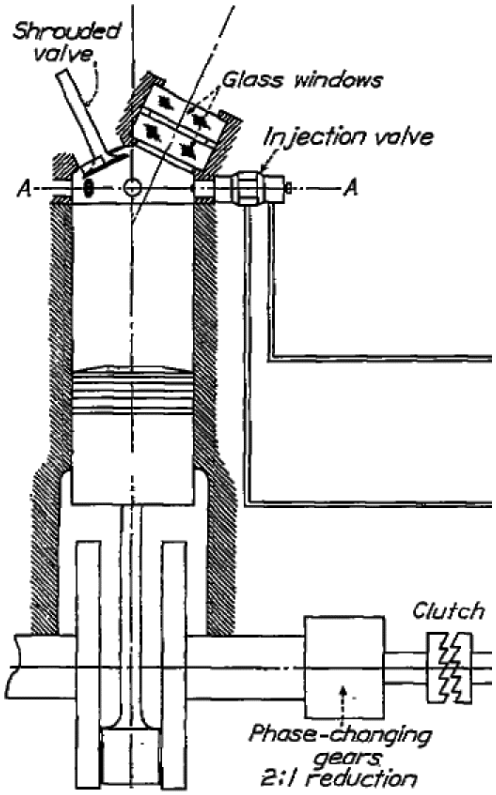


Figure 7. An early example of removing the exhaust valves to enable optical access in an overhead valve engine (Rothrock and Spencer [15])

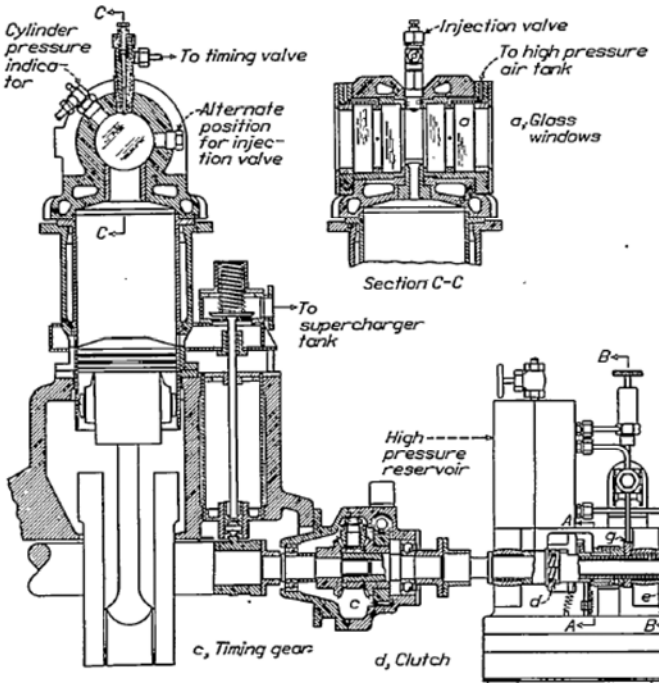


Figure 8. NACA's early optical diesel engine had a disk-shaped combustion chamber with glass side windows

produced with a fixed shroud orientation was found to be approximately proportional to engine speed.

Concurrently, the NACA group also investigated the impact of air flow on the combustion process [15]. For this work, the pent-roof engine geometry shown in Figure 6 was modified by removing both exhaust valves and replacing them with a large glass window (Figure 7). The engine was operated with only a single fuel injection event, and the two intake valves were used for both the intake and exhaust processes. Additionally, a mirror was placed atop the piston to enable Schlieren imaging of the combustion process through the head window. Both the images obtained and the in-cylinder pressure records showed that the highly reproducible swirling flows also resulted in the most reproducible combustion performance, clearly demonstrating the link between flow motion and cyclic variability in the combustion process. Work in the same engine, published shortly after the end of the war, captured images at 200,000 fps in order to examine the onset of engine knock [16]. Although this work was based on only a single-image sequence, it indicated that knock originated in partially-burned or auto-igniting gases and propagated as a wave at supersonic speeds. Still higher-speed imaging, at 500,000 fps, was performed at NACA in a two-stroke engine with a full-view glass window at the top of the combustion chamber [17]. Specific details regarding the engine were not made available; however, this work suggested the knock phenomenon was a multi-step process that started with auto-ignition in the end gases and was shortly followed by explosive, detonation-like waves that may originate at multiple sources.

**Compression ignition (diesel) engines**

Although the discussion so far has focused primarily on spark ignition engines, work was also proceeding towards obtaining a better understanding of diesel combustion through the use of optical engines. Due to the higher compression temperatures and pressures achieved in diesel engines, early optically accessible engines were highly modified. Rothrock and co-workers [18, 19] report measurements obtained in the early 1930's in the optical engine shown in Figure 8. In this engine, the combustion chamber was a vertical disk with transparent sidewalls, which allowed the fuel injection, vaporization, and combustion processes to be examined using a high-speed camera capable of up to 4000 images at rates up to 2000 fps. With a compression ratio of ~15:1 and peak (motored) cylinder pressures exceeding 30 bar, failure of the windows proved to be problematic and limited the amount of data that could be acquired, though steps were taken to minimize the thermal and pressure loading of the windows. This work showed that significant vaporization of the fuel could occur even during a short ignition delay period, and that excessive ignition delay led to combustion starting nearly simultaneously throughout the combustion chamber resulting in a violent combustion 'shock'. Combustion, as indicated by natural flame luminosity, was observed to begin around the periphery of the fuel jet before

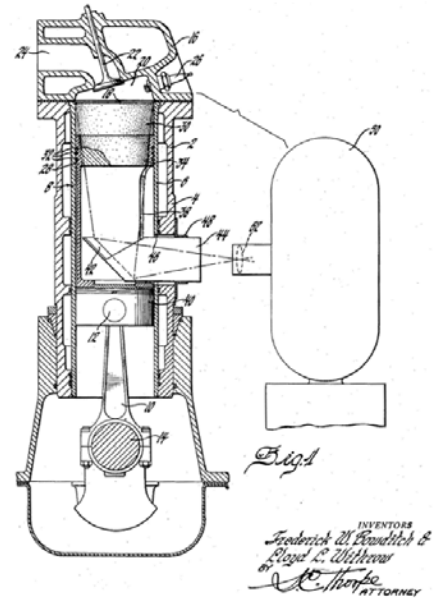


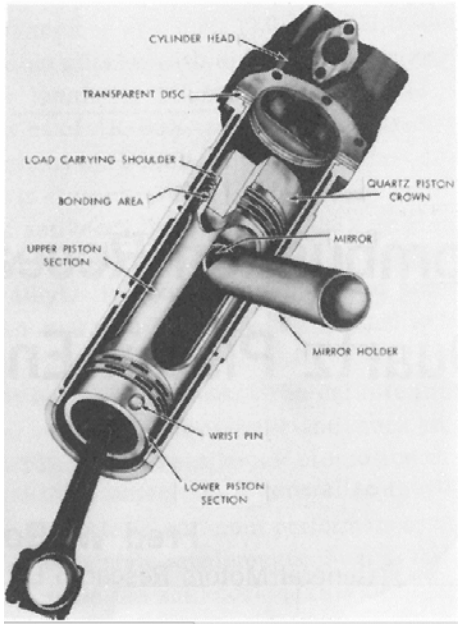


Figure 9. Schematic diagram of Bowditch's slotted, extended piston design from [20], and a 3-d rendition from [21].

spreading around the chamber. Optical diesel engines of similar design continued to be used for the next 6–7 decades.

## POST-WAR DEVELOPMENTS

### Spark ignition engines

With the exception of the two NACA papers published shortly after the end of the war [16, 17], optical reciprocating engine research apparently ceased during the 1940's and early 1950's.

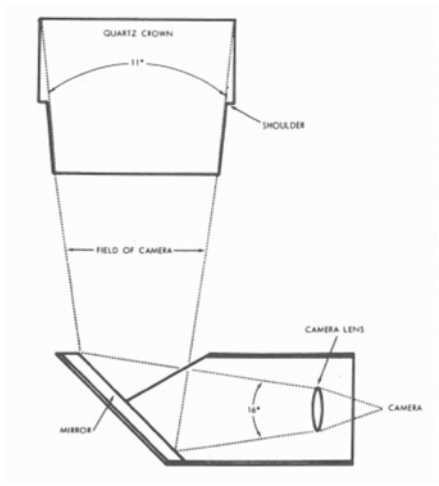


Figure 10. Bowditch's quartz piston top was designed to accommodate mechanical and thermal design requirements, as well as to maximize optical access

In 1958, however, F.W. Bowditch of the General Motors Corporation applied for a patent on the unique, optically accessible piston assembly shown in Figure 9 [20]. In many ways the design resembles the hollow extended piston assembly used by NACA in the 1930's [14]. However, Bowditch's essential innovation involved slotting the piston extension to allow the combustion chamber to be viewed from below via a 45° mirror and a quartz piston top. In this way, a large degree of optical access could be obtained in overhead-valve engine designs without significant modifications to the valve train or to the combustion chamber geometry. Bowditch [21] reports successfully operating this engine at compression ratios of up to 10.7:1 at engine speeds of 1200 rpm.

In developing his engine, Bowditch addressed many of the design challenges that optical engine designers still struggle with today. The shape and size of the quartz piston top, shown in Figure 10, was selected considering mechanical, thermal, and optical access requirements. A tapered quartz section was selected to maximize the viewing area. Accommodating this taper required the load-bearing shoulder to be placed lower than was required by mechanical strength considerations. The rings were also required to be low on the piston (see the illustration in the lower portion of Figure 9) where enough material was available to accommodate the ring groove, leading to a large top ring-land crevice – though not as severe as in the earlier NACA design. The quartz piston was bonded to the lower, metallic piston component using a high-temperature epoxy. Surprisingly, Bowditch makes no mention of efforts to select the lower piston material to minimize differential thermal expansion, which can add considerable stress to the bonding agent. Likewise, there is no report of difficulties in balancing the additional reciprocating mass. Provision was also made to admit light into the combustion chamber through a Pyrex® disk sandwiched between the liner and the head. However, breakage

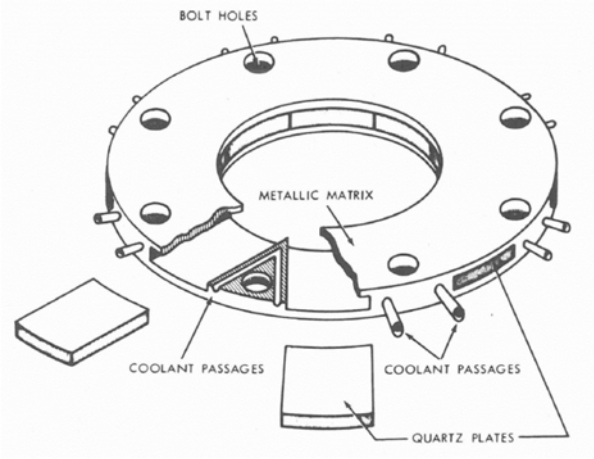


Figure 11. Laminated disk assembly developed to allow illumination of the combustion chamber through quartz windows in the upper cylinder walls

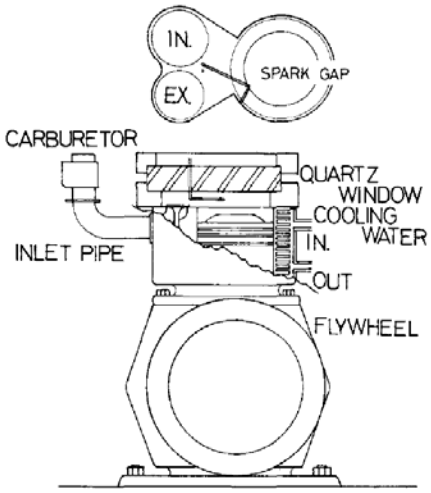


Figure 12. Nakanishi et al. incorporated a spark electrode into the optical window to allow for a more realistic spark location [22]

problems required replacement of the disk with a cooled, laminated assembly with discrete quartz windows (Figure 11).

The operational difficulties that Bowditch encountered with this engine are likewise familiar to modern researchers. Excessive oil leakage past the valve guides was found to eventually foul the mirror, a problem that was resolved with special valve stem seals. Likewise, oil coming up from the crankcase was problematic, and required a special ring-pack to resolve. Despite these difficulties, Bowditch was able to identify interesting behavior in this engine, including a slowing of combustion with decreased manifold pressure and more rapid combustion with increased compression ratio.

Post-war work in SI engines also continued in the side-valve engine configuration, which did not require the use of a Bowditch-style piston to achieve extensive optical access. An engine design incorporating a large quartz head-window, similar to that used by Rassweiler and Withrow [12], was employed by Nakanishi, et al. [22]. In contrast to earlier designs, however, this engine incorporated a spark electrode that passed through a hole drilled in the quartz window, providing a more central spark location – as shown in Figure 12. This engine was capable of fired operation for a sufficient period of time to enable the examination of the impact of EGR on the combustion process. Incorporating EGR into the intake charge of engines with a high degree of optical access remains a challenge even for modern optical engines.

Using methodology similar to that pioneered by Rassweiler and Withrow, Nakanishi et al. used both flame photographs and pressure analysis to investigate the impact of EGR, turbulence, and air-fuel ratio on flame propagation. Like Marvin and Best [5], they noted that EGR slowed combustion rates, but they also noted that EGR increased cyclic dispersion. High turbulence combustion chamber designs and richer fuel-air mixtures were found to promote early flame kernel propagation, increase the flame speed, and improve the cyclic dispersion.

**Compression ignition (diesel) engines**

At about the same time Bowditch published his work, optically accessible engines were also being employed in renewed efforts to understand diesel combustion. In 1962, Lyn and Valdmanis, using an engine modified to have a disk-shaped combustion chamber much like the NACA engine shown in Figure 8, obtained high-quality Schlieren images of a single fuel jet [23]. Lyn and Valdmanis found that, in general, evaporation of the fuel was far from complete at the time of ignition. They went on to argue that because the temperature and pressure at the end of compression are above the critical point values for many hydrocarbons, much of the fuel may be already in gas phase but with a density very close to that of liquid fuel. The lack of a distinct liquid-gas interface under diesel combustion conditions remains a very active area of research (*e.g.* [24]).

The first significant post-war advances in optically accessible diesel engines were reported by Ricardo & Co. Engineers (e.g. [25]). Their ported two-stroke engine allowed the installation of various pistons and heads, permitting optical investigations of both direct-injection (DI) and pre-chamber diesel designs (Figure 13) using a high-speed (up to 16000 fps) color camera. Either quartz or Perspex® (poly-methyl methacrylate, also known as Plexiglass®) windows were used. The Perspex® windows were found to withstand 10-20 engine firings before the surface was damaged, and soot deposited on the windows was easily cleaned between tests. In an early example of adopting special operating procedures to compensate for differences in combustion characteristics that may occur in optical engines, the engine was preheated by scavenging with air at 300°C. The scavenging air pressure was set to achieve near-TDC densities typical of naturally aspirated 4-stroke diesels.

Although few details of the optical engine hardware are provided, important insights into diesel combustion were obtained in this engine, including findings of DI spray impingement on combustion chamber surfaces, spray tip

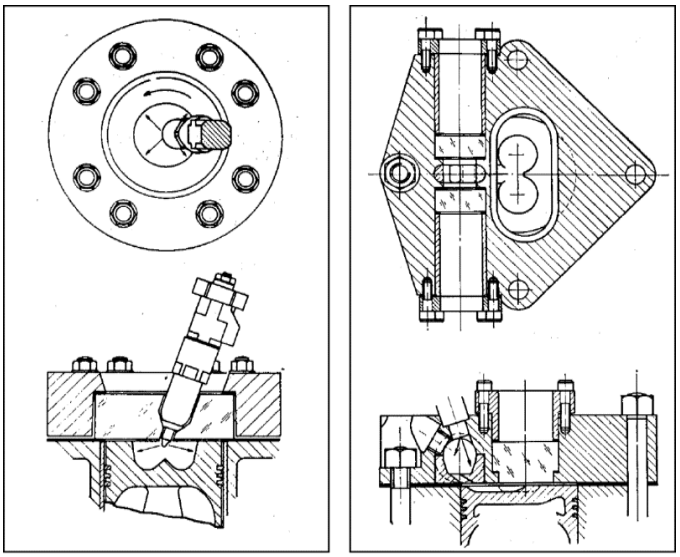


Figure 13. Ricardo's optically accessible diesel engine allowed investigation of both DI and pre-chamber concepts [25]

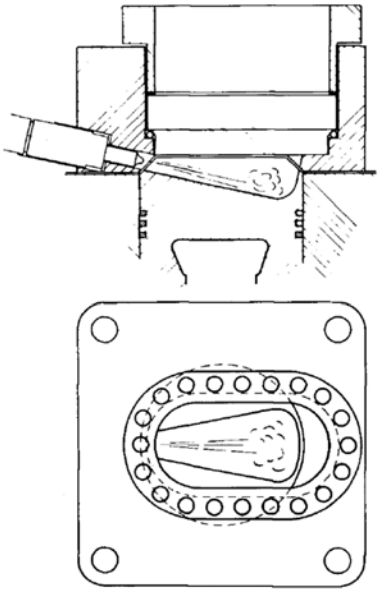

Figure 14. Ricardo's simulation of a sector of a large bore engine [25]

deflection by swirl, and significant soot formation with subsequent burn-out – leading to the observation that engine-out soot emissions may not be dominated by soot formation, but rather by the rate at which the soot formed mixes with additional air and oxidizes. With low cetane fuel (CN ~ 30) and low loads very little soot formation was observed, but as load increased soot luminosity increased and loud knock resulted. These latter observations are likely familiar to current-day diesel HCCI researchers.

Imaging of the cold-start ignition process also helped clarify the mechanism of glow-plug assisted ignition; ignition was observed in the fuel spray on the leeward side of the plug. Lastly, considerable effort was spent in trying to understand both the in-cylinder flows and the nature of combustion through development of various flow-indicating diagnostics and through doping the fuel with copper and halogens in order to roughly deduce flame temperatures from the color of the flame.

In a later publication [26] Ricardo engineers reported on measurements in an optically accessible engine designed to mimic a direct-injection, open chamber geometry more typical of large-bore engines. To accomplish this, they considered just a single spray penetrating into a combustion chamber shaped like a segment of a typical large-bore engine – see Figure 14. In order to achieve the required compression ratio using a smaller displacement base engine, they could not match the typical fuel-air ratio of the large bore engine, and the measurements were obtained under more fuel-rich conditions than was typical of a serial production engine. A major conclusion of this work, which in retrospect seems prophetic, was that the advancement of fuel injection capabilities to promote fuel-air mixing processes would be essential for the further refinement of near-quiescent, large-bore diesel engines.

## THE ONSET OF LASER-BASED DIAGNOSTICS

### Spark ignition engines

With the commercial availability of lasers in the 1970's optical engine studies increased significantly. Initially, laser-based diagnostics were focused largely on obtaining more quantitative velocity data than could be obtained using hot-wire anemometry or flow visualization techniques, and early work was performed in side-valve engines such as those employed by Ricardo [3] or Rassweiler and Withrow [12]. One example [27] used a single large quartz head window, through which laser Doppler velocimetry (LDV) measurements were performed in a backscatter configuration. The window was reported to require cleaning after approximately 5 minutes of run time.

A second example [28] used opposed windows in a spacer plate between the block and the head to enable forward-scattering LDV measurements. Unlike the earlier examples of opposed windows within the block (see Figure 4), the use of the spacer plate resulted in a significant decrease in compression ratio. A second embodiment, described in the same paper, allowed the investigation of 'torch' or pre-chamber ignition flows intended to facilitate lean operation. In this case, sapphire windows were installed in slots machined into the cylinder head.

Sapphire ($Al_2O_3$) has very favorable mechanical properties, with a tensile strength approaching that of cast irons and a Moh hardness of 9, which provides for excellent abrasion resistance. It retains its strength at high temperatures, and has a thermal expansion coefficient that is well-matched to stainless steels, thereby minimizing stresses caused by differential thermal expansion between the window and its mounting structure. On the other hand, as will be seen below, the relatively large thermal expansion can cause high thermally induced stresses

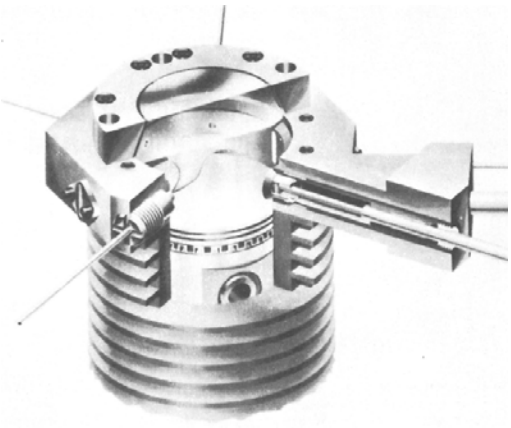

Figure 15. The side-valve engine introduced by Sandia National Laboratories in 1979 [29]

when temperature gradients exist within the window. The optical properties are also generally inferior to that of quartz. Sapphire has anisotropic optical properties and is birefringent, making it difficult to use with polarization sensitive diagnostic techniques. It may also contain chromium impurities which lead to high absorption in the near-UV and green-yellow portions of the spectrum, with subsequent emission in the red (694 nm, the wavelength of a ruby laser). The refractive index of sapphire is also significantly higher than quartz, leading to a greater amount of distortion when imaging is performed through curved window surfaces. Lastly, it has a density that is roughly twice the density of quartz, which can lead to balancing difficulties when sapphire is used in piston windows typical of a Bowditch piston design.

A new, simplified optical engine geometry used in a number of optical studies performed over approximately two decades was introduced in 1979 by researchers at Sandia National Laboratories [29]. This engine was based on a commercial overhead valve engine that was modified to place the valves in the cylinder wall, as illustrated in Figure 15. To prevent the piston rings from running over the valves a relatively large clearance height was required, and a CR of only 5.7:1 was achieved. Nevertheless, with this valve configuration, the quartz or sapphire head window provided a clear aperture of 71 mm into a cylinder with a bore of 76 mm. Additional access ports in the upper liner segment containing the valves provided additional optical access or could be fitted with a fuel injector or spark plug. Moreover, by shrouding the intake valve, the in-cylinder swirl ratio could be varied over a range from 0 to over 8. The engine could run motored for long periods of time and could be fired continuously at speeds up to 1800 rpm. Although the intake flows generated by the unusual valve configuration and the 'pancake' combustion chamber geometry were clearly atypical of commercial engines, the extensive optical access and geometric simplicity was anticipated to facilitate both the experiments and the development of computational models.

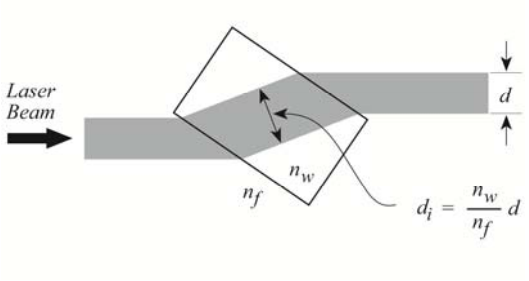


Figure 16. Windows mounted at Brewster's angle can reduce energy losses due to reflections and allow higher beam fluence due to the increased beam diameter within the window material. Figure adapted from [43].

Over the course of several years, a great number of studies performed in this engine, using a wide variety of laser diagnostic techniques, shed light on:

1) The typical form of the radial profiles of swirl velocity and the decay of the swirl velocity (providing information on the boundary layer structure) [29], as well as direct measurements of velocity and temperature within the boundary layer [30, 31]
2) The linear scaling of both mean and turbulent velocities with engine speed [29]; highly anisotropic turbulence, with both normal and shear stresses scaling with engine speed [32]
3) Clear confirmation of swirl center offset and precession of the swirl axis about the cylinder axis, as well as the ability of fuel jets to modify the swirl structure [29]
4) A tendency for turbulence to fall off rapidly at larger radii in swirling flows [33] while still removed from the wall.
5) Slow mixing of gaseous fuel jets, leaving both rich regions and regions too lean to support ignition even 40° aSOI [29, 34]
6) Flow/ flame interactions leading to anisotropic turbulence generation [35, 36], preferred swirl ratios for rapid combustion [33, 37], increasing turbulent flame wrinkling with increasing engine speed [38], and little turbulence production in the end-gas region [39]
7) Direct measurement of the turbulent burning velocity [40]
8) Visualization of HC leaving the ring-land crevice [41]
9) The ability of swirl to significantly impede mixing of the fresh charge with the internal residual gases [42].

In the latter study, the side-wall windows were mounted at Brewster's angle, an innovation that helps enable optical diagnostic techniques requiring high laser fluence – such as Raman scattering or multi-photon laser-induced fluorescence (LIF) techniques. In addition to minimizing surface reflections for p-polarized light, by mounting the windows at the Brewster angle the beam diameter within the window material is increased by the ratio of the refractive index $n_w$ of the window material to that of the surrounding fluid $n_f$ (see Figure 16),

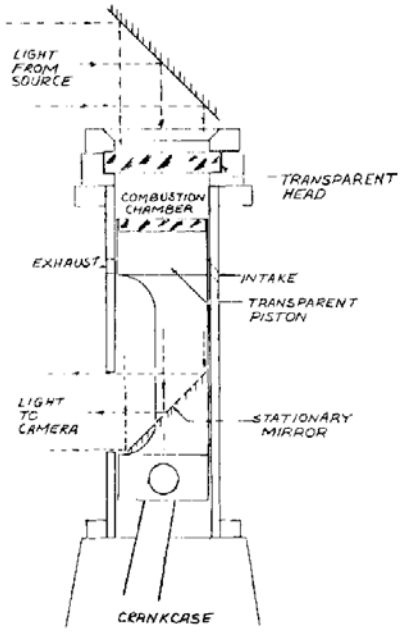


Figure 17. The ported, two-stroke engine employed by Princeton researchers for approximately two decades [44]

allowing higher energy laser pulses to be transmitted without window damage [43].

Concurrent with the introduction of the Sandia side valve engine, researchers at Princeton University introduced a very flexible, ported design incorporating a Bowditch-style extended piston [44] – see Figure 17. This engine allowed optical access through either a large head window, a piston window, a quartz spacer ring between the block and the head [45], or side-windows surrounding a bowl or cup in the head (see, *e.g.* [46]). A CR of up to 16:1 and a maximum speed of 4000 rpm were anticipated by the designers, although in practice the speed appears to have been limited to 3000 rpm. Interchangeable inserts in the ports allowed the TDC swirl ratio to be varied from approximately 0 to 6, depending on the scavenging ratio. An oil control ring at the lower end of the piston was used to keep the mirror clean, and three bronze-impregnated Teflon (a material commonly used in oil-free compressors) compression rings were used near the piston top.

The Princeton engine was subsequently used to investigate a number of in-cylinder phenomena. Examples include:

1) The impact of resonant pressure waves and engine speed on the port flows [47]
2) How engine speed affects the structure of hollow-cone fuel sprays and fuel-air mixing in swirling flows [48]
3) Visualization and quantitative measurements of liquid and vapor fuel distributions using a variety of injectors and injector configurations, injection pressures, swirl ratios, engine speeds and diagnostic techniques [45, 46, 49-51]
4) In-cylinder droplet sizing [46]
5) Measurements of turbulent velocity and length scales (both direct and using Taylor's hypothesis) and the anisotropy of these scales [52-56]. These measurements helped establish the insensitivity of TDC turbulence levels to the intake flows, confirmed the scaling of turbulent velocities with engine speed, demonstrated that turbulence was increased by flame passage but rapidly decayed, and found that – like homogeneous charge engines – cyclic variability was reduced with flow swirl in direct-injection engines, also.
6) Two and three-dimensional visualization of turbulent flame structure and how it is impacted by mixture stoichiometry and engine speed was also performed [57, 58]. No discrete 'islands' of unburned mixture were observed, though the existence of peninsulas that could be misinterpreted as islands were observed in 2-d images, especially for lean mixtures and high engine speeds. This work showed that flame wrinkling increases for lean mixtures and with increased engine speed, such that flame area (and combustion rate) scales with piston speed at sufficiently high speeds.
7) The impact of piston bowl shape and position on turbulent flow structure [59].

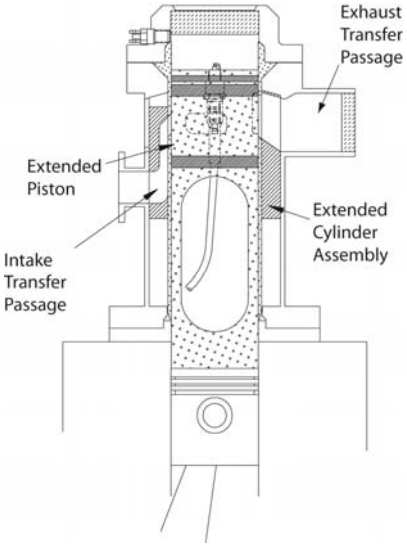


Figure 18. Sandia's ported, two-stroke engine [60]

Approximately a decade later, a very similar optically accessible two-stoke was introduced by researchers from Sandia National Laboratories [60] that was used to investigate scavenging processes in two-strokes [61, 62]. In the latter study, optical access through the piston was not required, and access through the Bowditch piston was employed to enable the use of a central spark location (Figure 18). In contrast to the Princeton engine, this engine employed piston rings made from a graphite-filled polyimide (Vespel®), which allows higher temperature operation than Teflon-based rings.

An optically accessible two-stroke engine without an extended piston assembly, employing a large, flat head window has also been employed by Daimler-Benz for the study of knock [63, 64].

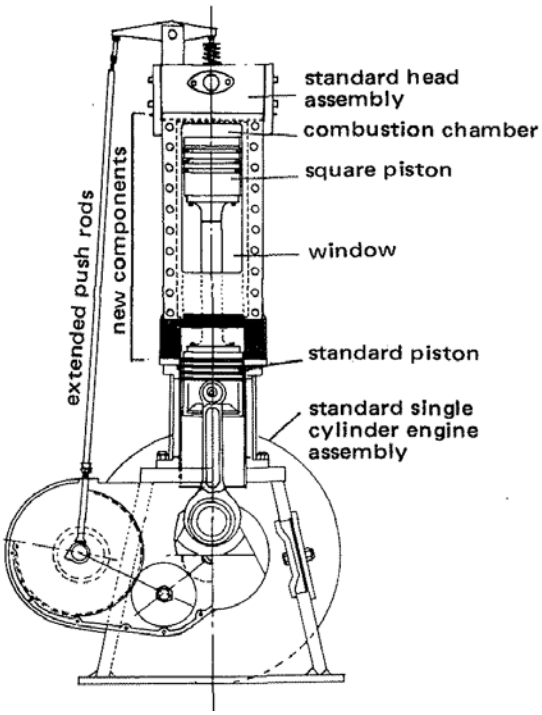


Figure 19. MIT's square piston engine introduced in 1980

In a very significant departure from conventional engine geometries, Namazian and co-workers at the Massachusetts Institute of Technology (MIT) introduced in 1980 the square piston engine shown in Figure 19. This engine achieved extensive optical access through two opposed cylinder walls made of quartz. 'Rings' were constructed from linear segments, with overlapping joints at the corners; coil springs behind the segments helped promote sealing. Several different ring materials were explored, including several varieties of filled Teflon®. However, hard graphite ring material proved most successful for maintaining clean windows. Like the Bowditch-piston designs discussed above, special measures (a felt seal) were required to keep oil from the lower crankcase from contaminating the extended piston/cylinder assembly.

The engine had a CR of 4.8:1, was run at a speed of 1380 rpm, and was fired in short bursts of approximately 16 cycles. After approximately 3 fired cycles the combustion was reasonably stable. Similar 'burst' firing strategies to obtain stable operation or desired surface temperatures in optical engines have been subsequently employed by others (*e.g.*, [62, 65, 66]).

In addition to numerous observations of the flame initiation and propagation process, the extensive optical access through the cylinder walls provided by the square piston engine allowed observation of several in-cylinder phenomena that had not previously been observed. During intake, vortices in the cylinder corners formed by the cylinder walls and the head were generated by the intake flow. Although these vortices had been seen previously in water analog engines [67], here they were found to persist throughout the compression stroke and potentially to impact the flame propagation process. This engine also allowed the direct observation of ring-land crevice flows during expansion, which can be a significant source of unburned HC emissions. Lastly, during the exhaust stroke the piston was found to scrape the HC-rich boundary layer along the cylinder wall into a vortex in the corner between the piston top and the wall, a process that had also been previously visualized in a water analog device [68].

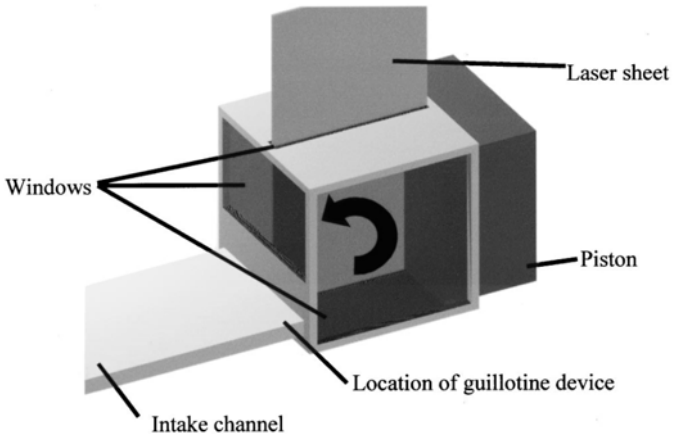


Figure 20. The square piston engine employed by the Institut de Mécanique des Fluides to generate a nearly 2-dimensional tumble vortex [74]

A similar square piston engine was subsequently introduced by Daimler-Benz in 1990 [69]. In contrast to the MIT engine, in the Daimler-Benz engine all four cylinder walls were formed from quartz plates. The engine achieved a CR of 10:1, could be fired in bursts of 250 cycles, and had a rated speed of 2500 rpm. This engine was fruitfully employed to examine the statistics of wrinkled engine flames to obtain data in support of turbulent combustion models [69, 70], fuel-air mixing studies employing LIF techniques [71], cinematic PIV studies at flame rates of 200 Hz [72], and in-cylinder imaging of NO and temperature fields [73].

The Institut de Mécanique des Fluides in Toulouse has also used a square engine geometry [74, 75] to examine the breakdown process of a tumble vortex and to study the interaction of fuel jets on the vortex evolution and breakdown [76]. In this low CR (4:1), low-speed (206 rpm) device an inlet channel spanning practically the full 'bore' generated a nearly ideal, two-dimensional tumble vortex. A guillotine-like device served as the intake valve (Figure 20). Notable conclusions from this work include the significant turbulence production associated with the compression process and the potential for jet-vortex interactions to significantly decrease turbulence levels near TDC.

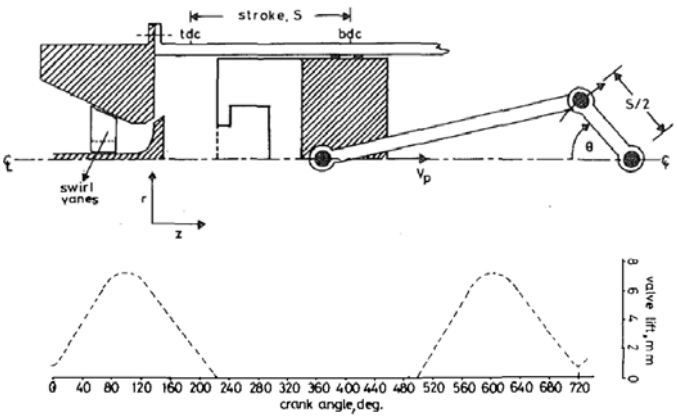


Figure 21. The transparent cylinder engine model engine from Imperial College. Figure adapted from [77]

Subsequent advances to optical engine technology were made in the mid-1980's by implementing full cylindrical transparent liners similar to that used by NACA in 1939 [14]. In 1982 researchers from Imperial College [77, 78] used a single-cylinder model engine with a compression ratio of 3.5:1, constructed from a Plexiglass® cylinder (Figure 21). The engine was designed for motored in-cylinder flow studies, and featured a single, central valve that was used for both the intake and the exhaust processes. Removable swirl vanes in the port allowed both quiescent flows as well as flows with a swirl ratio of approximately 2.5, typical of production diesel engines, to be investigated. Although this engine was clearly atypical of production engines in many respects, and the studies were conducted at low speed (~200 rpm), work conducted in this engine and in a similar engine with a stationary valve provided quantitative data characterizing engine valve flows that is still used by engine flow modelers for validation of their simulations.

In 1984 Richman and Reynolds described the development of the transparent cylinder research engine at Stanford University pictured in Figure 22 [79]. This engine was specified to have a compression ratio that could be varied from between 6.25 – 11, and a speed capability up to 3000 rpm. The innovative features of this engine were the early use of electro-hydraulic valve actuators and the thin-walled transparent cylinder fabricated from single-crystal sapphire. Using a simple heat transfer model, Richman and Reynolds showed that while the mechanical hoop stresses in the cylinder wall decreased with increasing cylinder wall thickness, the thermal stresses increased. Under the assumptions used in their model, the total stress was minimized with a wall thickness of just 4.45 mm. Sealing at the upper and lower surfaces of the sapphire cylinder was accomplished using silver-plated metal o-rings.

In contrast to the earlier, ring-less NACA design, this engine employed carbon-filled Teflon® rings, which were reported to leave the cylinder walls free of deposits. The piston operated with a 0.5 mm clearance between the piston and the cylinder walls, and was centered in the bore by alignment bushings (also called 'rider' rings). No special accommodation

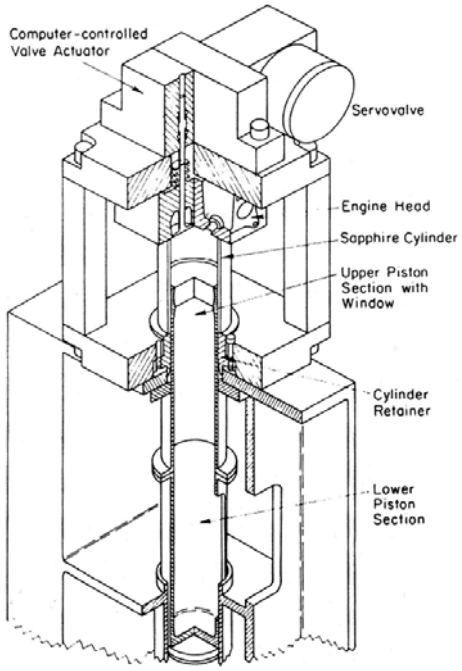


Figure 22. The transparent cylinder engine developed at Stanford University [79]. Although not readily apparent from the figure, the lower piston section was slotted to allow viewing using a Bowditch-like mirror assembly.

appears to have been made for axial thermal expansion of the sapphire cylinder.

Studies performed in this engine demonstrated significant interactions between the intake jets and the piston top, the existence of a strong ring-land crevice jet aligned with the ring gap, and indications of the roll-up vortex observed in the square-piston MIT engine.

The Stanford engine was followed closely thereafter by transparent cylinder engines from Ford [80], the NASA Lewis Research Center [81], and General Motors [66]. Like the Stanford engine, the Ford engine featured a Bowditch piston assembly. Although it was designed to run only at low speed, dynamic similarity was attained by running the engine with an operating fluid of compressed Freon. The NASA engine (Figure 23) was likewise a low-speed device (~300 rpm), designed for motored use only. It had a compression ratio of 3.3:1, featured a quartz cylinder 6.4 mm thick, and induced axisymmetric flows through the use of a single valve for both intake and exhaust. Despite the limitations of this engine, it provided useful information regarding potential 'flapping' motion of the intake jets and confirmed the existence of outflows from the ring-land crevice during expansion.

The offering from General Motors was capable of more realistic operating conditions. Like the Stanford engine, it used a sapphire liner with a thickness of 5 mm. However, the engine could be motored at speeds up to 4000 rpm with the nominal compression ratio of 9:1. The main innovations incorporated in this engine were in the design of the liner 'nest', which

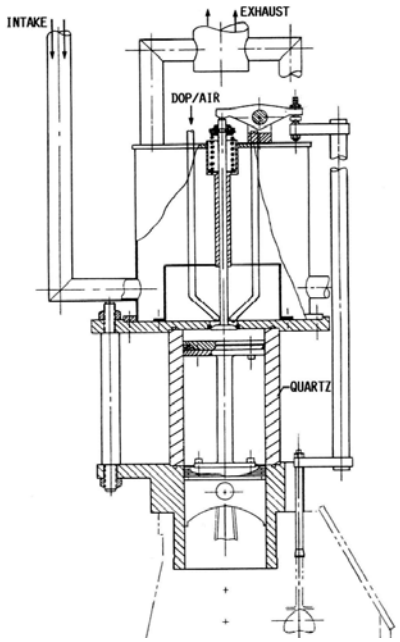


Figure 23. NASA Lewis's transparent engine featured a single, central valve and was used to examine flow structure under motored operation [81]

thermally isolated the liner from the head, provided for active piston cooling to reduce heat transfer to the liner, and pneumatically supported the liner such that the vertical force was independent of liner temperature and thermal expansion. A schematic of the liner nest is shown in Figure 24.

Like the square-piston MIT engine, graphite piston compression rings were used, though additional tension was supplied by Inconel® backing spring-rings. At the lower end of the piston, scraper rings and an oil control ring were used to prevent the escape of oil from the crankcase. Research conducted in this engine included velocity measurement using a form of particle tagging velocimetry, low-speed flow visualization, and flame imaging studies – confirming earlier observations of intake jet flapping and significant cycle-to-cycle variability in the combustion development.

Due largely to the expense of full transparent liners, a number of researchers chose instead to employ a transparent ring of limited height for the upper portion of the liner (*e.g.*, [82]). Retaining a metallic lower portion also has the advantage of allowing for liner cooling. Because the rings are positioned so that they do not pass over the transparent ring, harder ring materials or higher ring tension can also be employed. The disadvantage to this arrangement is the larger top ring-land crevice. In addition, due to the limited height of the quartz ring, it is easier to allow for thermal expansion without incorporating a pneumatic 'nest'. Thermally stable Grafoil® flexible-carbon gasket material has the appropriate release response to accommodate differential thermal expansion. In the design shown in Figure 25, a thin (0.25 mm) gasket was used on the

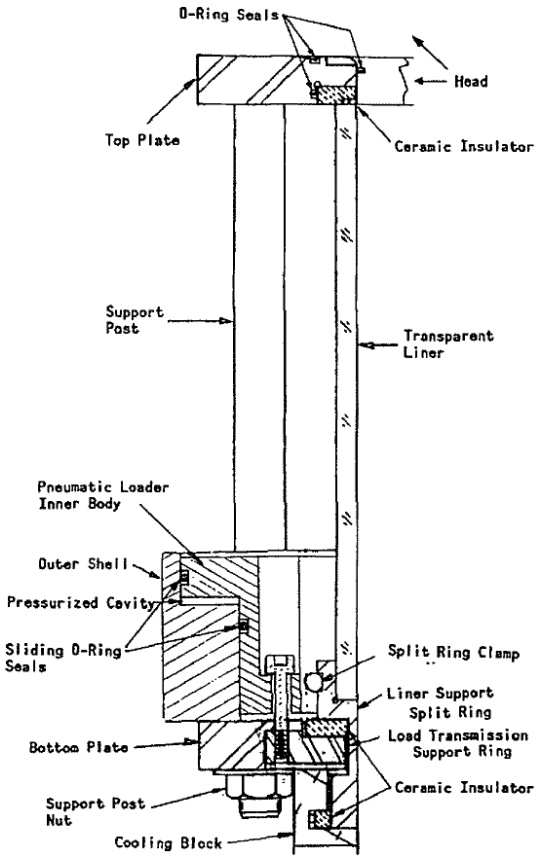


Figure 24. The liner 'nest' design employed by General Motors [66]

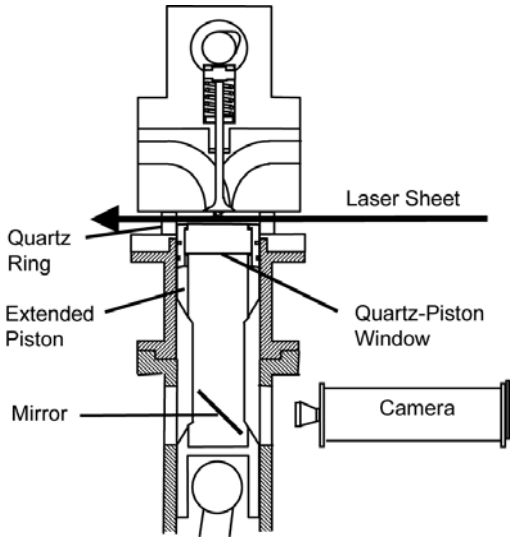


Figure 25. An example of an optical engine incorporating a short, quartz ring into the upper liner [82]

lower end of the quartz ring, while a thicker gasket (3 mm) was used on the upper ring [83].

A homogeneous charge (port-injected) engine incorporating gable windows (Sandia National Laboratories)

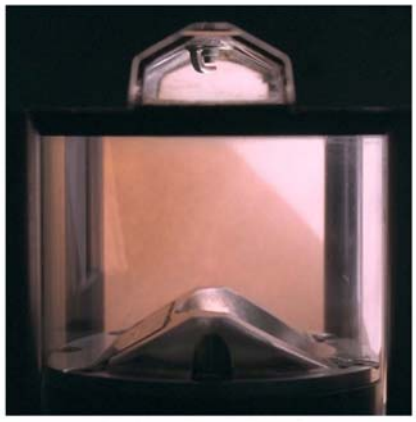

An example of gable windows in a direct-injection SI engine (Lund University)

Figure 26. Optical windows in the gables of the head enable access to the upper combustion chamber and the spark gap.

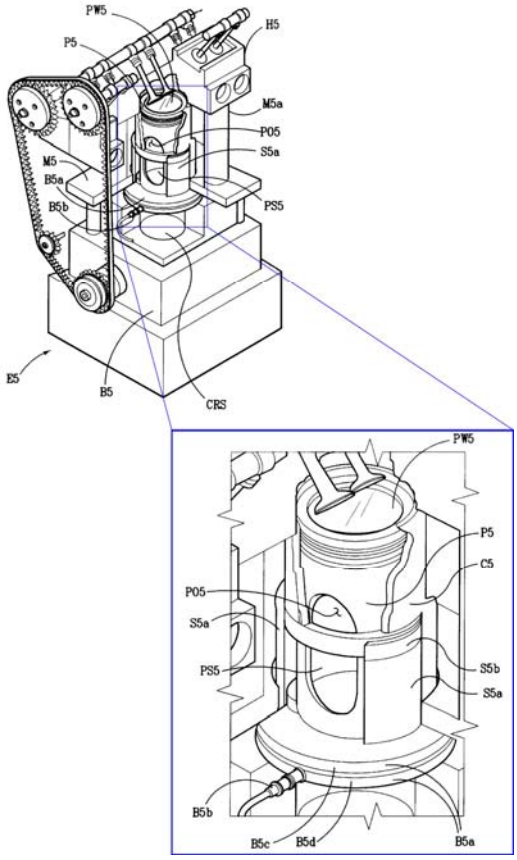


Figure 27. Sunnarborg's drop-down liner concept.

Although this design does not allow extensive optical access into the swept volume, velocity measurements obtained in this engine have helped clarify the impact of swirl on the spatial structure of the in-cylinder turbulence (confirming the rapid decay of fluctuations at larger radii previously measured in [33]) and has reinforced earlier observations of the stabilizing effect of swirl on the in-cylinder flow. The engine has also been effectively employed to obtain quantitative data for code validation [84, 85].

A drawback to the transparent liner designs described above is the lack of optical access into the combustion chamber of pent-roof designs. This drawback was soon rectified by placing optical windows into the 'gables' of the engine head. An early example is the Bowditch-piston optical engine used by the Institut Français du Petrole (IFP), which, in conjunction with CFD modeling, helped to clarify the tumbling flow structure formed by four-valve engines with twin intake ports [86]. The IFP engine did not use a transparent liner. However, several other groups later implemented both gable windows and transparent liners – examples are shown in Figure 26.

In 1993 Espey and Dec [87] introduced an optically accessible diesel engine that facilitated optical engine research significantly: a quick release, 'drop-down' liner that enabled rapid access to the combustion chamber for cleaning, without the need to remove the head and associated plumbing and drive mechanisms. This engine was quickly adapted for light-duty SI applications by Sunnarborg [88], who coupled the drop-down liner concept of Espey and Dec with the liner nest concept of Bates – as shown in Figure 27.

In the Sunnarborg design, when the liner (C5) is in the raised position it is supported by a cylindrical cradle with two ears (S5b), which in turn are engaged by supports (S5a) attached to a base plate (B5a). The base plate forms the upper half of a hydraulically operated lift, which upon pressurization maintains a constant upward force on the liner – functioning much like the pneumatic loader seen in Figure 24. When the hydraulic pressure is released, the base descends approximately 1 mm, allowing the cradle to be rotated 90°. In this position the cradle ears are no longer above the supports, and the liner can be lowered to provide access to the combustion chamber. The ability to easily and quickly access the combustion chamber for cleaning is essential if sufficient optical measurements are to be made to be of engineering value. A drop-down or quickly removable liner concept is now an integral part of most modern optically accessible engines.

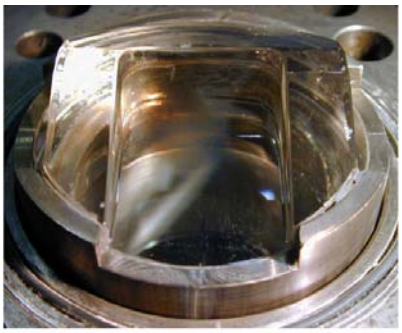

Quartz piston top employed for studies of spray-guided direct-injection combustion systems

Distorted view of the cylinder head through the piston

Figure 28. An example of a complex piston shape. Photos courtesy of Mattias Richter, Lund University.

With excellent optical access to the entire combustion chamber, and the ability to rapidly clean the optical windows, the next step toward making the most realistic engine measurements involved adopting piston shapes matching prototype or production engines. Complex piston shapes were first adopted for the diesel engines discussed below, but as wall-guided, direct-injection gasoline engines began to be developed these piston shapes were also adopted. Such shapes can be accurately produced using numerically-controlled grinding processes. An example can be seen in Figure 28. Note that these complex piston geometries cause significant image distortion, which can present considerable challenges when quantitative measurements are desired.

To close this section, we consider two of the optical engines developed more recently for SI combustion studies, one by Lotus Engineering, Ltd. in conjunction with Loughborough University [89] and the second by Toyota Central R&D Labs [90]. The contribution from Lotus/Loughborough has features similar to the Stanford engine shown in Figure 22, though much more refined. In its latest form (Figure 29), it features the hydraulically actuated Lotus Active Valve-Train system, such that there is no obstruction from a timing belt assembly. Additionally, as shown by the inset in the lower half of the figure, the transparent liner and head gable windows are incorporated into a single piece, providing seamless access to the combustion chamber. Tests conducted with bronze and molybdenum filled PTFE compounds, PTFE coated metal, and

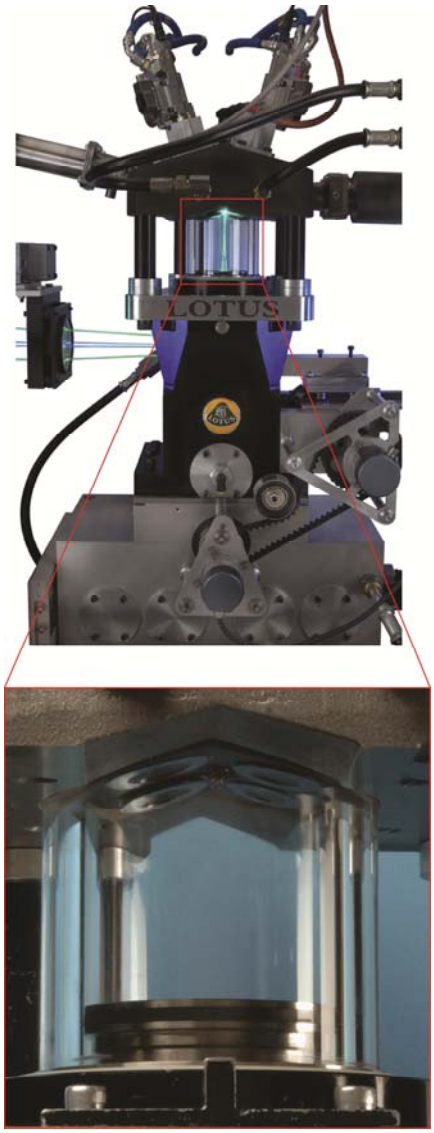


Figure 29. The high-speed optical engine developed by Lotus Engineering, Ltd. and Loughborough University [89]

solid PTFE rings demonstrated that these compounds could not survive at high speeds and ring tensions, and a carbon-matrix ring material was used.

Design targets for this engine were a maximum cylinder pressure of 60 bar and a maximum speed of 5000 rpm. To achieve this speed, the crankcase required both primary and secondary balancing shafts, in addition to careful attention to the minimization of the reciprocating mass. To allow for rapid cleaning, the cover plates in the upper crankcase can be removed to give access to the piston wrist pin. Pushing the pin out allows the piston to be pushed down into the crankcase, enabling the liner to be removed. Disassembly, cleaning and reassembly can be done within 15 minutes.

To enable still higher speeds, the Toyota design abandoned the usual balancing approach, and implemented a system based on twin, vertically-opposed pistons shown in Figure 30. In

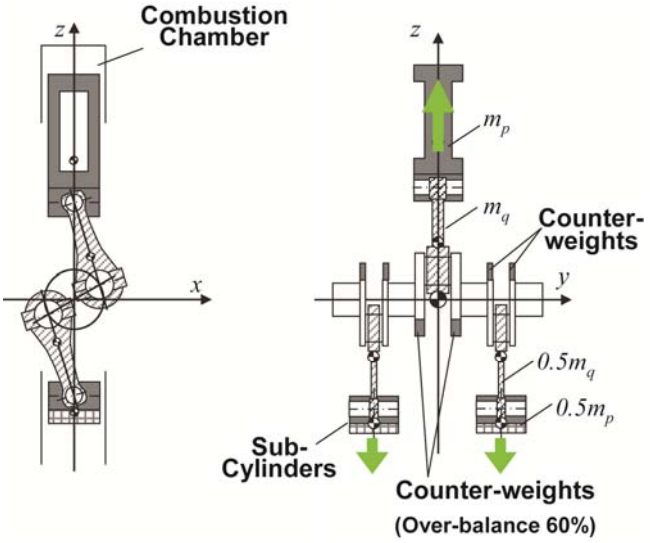


Figure 30. The vertically opposed balancing system implemented by Toyota Central research and Development [90]

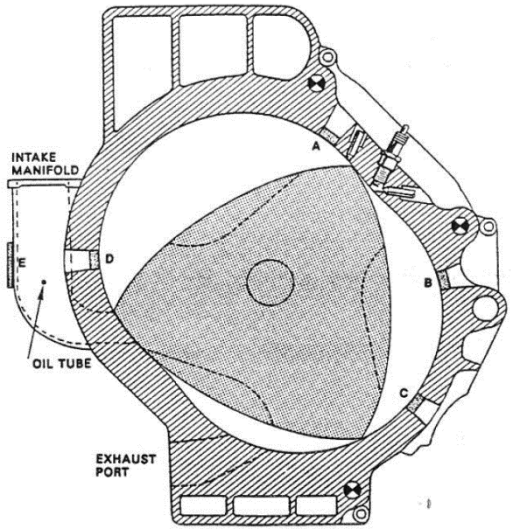


Figure 31. Modification of a John Deere rotary engine to permit measurement of gas velocities in the compression zone (window A), expansion zone (window B), exhaust zone (window C) and intake zone (windows D and E).

addition to balancing the engine, this system allows the minimization of the bending forces on the crankshaft. Like the Lotus design, the cylinder was shaped to incorporate the gables necessary for optical access into the upper combustion chamber. In addition, the Toyota engineers selected high-strength, over-sized connecting rod bolts and coated the inside of the cylinder with an unspecified coating to enable high-speed, un-lubricated operation. With these measures, high-quality optical images of the flame development could be obtained at 5000 rpm.

Space did not permit a complete listing of the many optical engines that have enabled significant advances in our knowledge of SI combustion over the last two decades. However, we encourage the reader to examine the following additional references for a sampling of the understanding that has been attained: [91-98]

**Optically-accessible production engines**

As noted in the introduction, there has been a great deal of work performed in production engines that have been modified to provide some degree of optical access. While in general a description of these modifications is beyond the scope of this work, we make one exception: the single example of a modification to a rotary engine to permit optical investigations shown in Figure 31. In 1988 Dimplefeld & Witze [99] report on the installation of windows in the trochoid of a production rotary engine to enable velocity measurements. The results indicated a very complex flow field, with relative turbulent intensities of approximately 50%. Over the relatively small range of engine speeds investigated, flow velocities (both mean and fluctuating) were observed to scale with engine speed.

## SUMMARY

Optically-accessible engines have a rich history of providing insight into the physics governing the fuel-air mixing, combustion, and emissions formation processes in internal combustion engines. In the 142 years that passed from Otto's first, hand-cranked model engine to the latest high-speed, high-pressure engines, optically accessible engines have provided new, detailed information that has helped enable the advancement and design of new, clean and efficient internal combustion engines. As computational capabilities increase, simulations are able to provide more and more understanding into the processes occurring within the cylinder of operating engines. We may eventually reach a point where these simulations will allow a full, accurate picture of the in-cylinder processes and how they can be optimized. However, for the next several decades, optically accessible engines will remain a valuable tool supporting engine research and development.

## ACKNOWLEDGMENTS

Support for this work was provided by the United States Department of Energy Office of Vehicle Technologies. This study was performed at the Combustion Research Facility, Sandia National Laboratories in Livermore, California. Sandia is a multi-program laboratory operated by Sandia Corporation, a Lockheed Martin Company, for the United States Department of Energy's National Nuclear Security Administration under contract DE-AC04-94AL85000.

## REFERENCES

1. Amann, C.A., *A perspective of reciprocating-engine diagnostics without lasers.* Progress in Energy and Combustion Science **9** (3): pp. 239-267, 1983.
2. Clerk, D. "Cylinder Actions in Gas and Gasoline Engines," SAE technical paper 210043, 1921.

3. Ricardo, H.R., *Some Notes on Gasoline-Engine Development*, in *NACA Technical Memorandum #420,* 1927.
4. Glyde, H.S., *Experiments to Determine Velocities of Flame Propagation in a Side Valve Petrol Engine.* J. Inst. Pet. Technol. **16**: pp. 756-776, 1930.
5. Marvin, C.F. and Best, R.D., *Flame Movement and Pressure Development in an Engine Cylinder*, in *NACA Report #399,* 1932.
6. Withrow, L. and Boyd, T.A., *Photographic Flame Studies in the Gasoline Engine.* Industrial and Engineering Chemistry **23** (5): pp. 539-547, 1931.
7. Withrow, L. and Rassweiler, G.M., *Spectroscopic Studies of Engine Combustion.* Industrial and Engineering Chemistry **23** (7): pp. 769-776, 1931.
8. Withrow, L. and Rassweiler, G.M., *Absorption Spectra of Gaseous Charges in a Gasoline Engine.* Industrial and Engineering Chemistry **25** (8): pp. 923-931, 1933.
9. Withrow, L. and Rassweiler, G.M., *Formaldehyde Formation by Preflame Reactions in an Engine Spectroscopic Study.* Industrial and Engineering Chemistry **26** (12): pp. 1256-1262, 1934.
10. Watts, S.S. and Lloyd-Evans, B.J., *The measurement of flame temperatures in a petrol engine by the spectral line-reversal method.* Proceedings of the Physical Society (London) **44**: pp. 444-449, 1934.
11. Hershey, A.E. and Paton, R.F., *Flame Temperatures in an Internal Combustion Engine Measured by Spectral Line Reversal.* University of Illinois Bulletin No. 262 **31** (9), 1933.
12. Rassweiler, G.M. and Withrow, L., *High-Speed Motion Pictures of Engine Flames.* Industrial and Engineering Chemistry **28** (6): pp. 672-677, 1936.
13. Rassweiler, G.M. and Withrow, L. "Motion Pictures of Engine Flames Correlated with Pressure Cards," SAE technical paper 380139, 1938.
14. Lee, D.W., *A study of air flow in an engine cylinder*, in *NACA-TR-653,* 1939.
15. Rothrock, A.M. and Spencer, R.C., *The influence of directed air flow on combustion in a spark-ignition engine*, 1939.
16. Miller, C.D., Olsen, H.L.*, et al.*, *Analysis of spark-ignition engine knock as seen in photographs taken at 200,000 frames per second*, 1946.
17. Male, T., *Photographs at 500,000 frames per second of combustion and detonation in a reciprocating engine.* Symposium on Combustion and Flame, and Explosion Phenomena **3** (1): pp. 721-726, 1948.
18. Rothrock, A.M. and Waldron, C.M., *Fuel vaporization and its effect on combustion in a high-speed compression-ignition engine*, 1933.
19. Rothrock, A.M. "Photographic Study of Combustion in Compression-Ignition Engine," SAE technical paper 340094, 1934.
20. Bowditch, F.W., "Cylinder and Piston Assembly," in US Patent App. 2,919,688, 2,919,688,
21. Bowditch, F.W. "A New Tool for Combustion Research A Quartz Piston Engine," SAE technical paper 610002, 1961.
22. Nakanishi, K., Hirano, T.*, et al.* "The Effects of Charge Dilution on Combustion and Its Improvement-Flame Photograph Study," SAE technical paper 750054, 1975.
23. Lyn, W.T. and Valdmanis, E., *The Application of High Speed Schlieren Photography to Diesel Combustion Research.* Journal of Photographic Science **10**: pp. 74-82, 1962.
24. Dahms, R.N. and Oefelein, J.C., *On the transition between two-phase and single-phase interface dynamics in multicomponent fluids at supercritical pressures.* Physics of Fluids **25** (092103), 2013.
25. Alcock, J.F. and Scott, W.M. "Some More Light on Diesel Combustion," SAE technical paper 640446, 1964.
26. Scott, W.M. "Looking in on Diesel Combustion," SAE technical paper 690002, 1969.
27. Rask, R.B. "Laser Doppler Anemometer Measurements in an Internal Combustion Engine," SAE technical paper 790094, 1979.
28. Asanuma, T. and Obokata, T. "Gas Velocity Measurements of a Motored and Firing Engine by Laser Anemometry," SAE technical paper 790096, 1979.
29. Johnston, S.C., Robinson, C.W.*, et al.* "Application of Laser Diagnostics to an Injected Engine," SAE technical paper 790092, 1979.
30. Foster, D.E. and Witze, P.O. "Velocity Measurements in the Wall Boundary Layer of a Spark-Ignited Research Engine," SAE technical paper 872105, 1987.
31. Lucht, R.P. and Maris, M.A. "CARS Measurements of Temperature Profiles Near a Wall in an Internal Combustion Engine," SAE technical paper 870459, 1987.
32. Foster, D.E. and Witze, P.O., *Two-Component Laser Velocimeter Measurements in a Spark Ignition Engine.* Combustion Science and Technology **59** (1-3): pp. 85-105, 1988.
33. Witze, P.O., *The Influence of Air Motion Variation on the Performance of a Direct Injection Stratified Charge Engine*, I. Mech E. C394/80. p. 25-31, 1980.
34. Johnston, S.C. "Precombustion Fuel/Air Distribution in a Stratified Charge Engine Using Laser Raman Spectroscopy," SAE technical paper 790433, 1979.
35. Martin, J.K., Witze, P.O., and Borgnakke, C. "Combustion Effects on the Preflame Flow Field in a Research Engine," SAE technical paper 850122, 1985.
36. Witze, P.O., Martin, J.K., and Borgnakke, C. "Fluid Motion during Flame Propagation in a Spark Ignition Engine," SAE technical paper 840377, 1984.
37. Witze, P.O. "The Effect of Spark Location on Combustion in a Variable-Swirl Engine," SAE technical paper 820044, 1982.

38. Smith, J.R. "Turbulent Flame Structure in a Homogeneous-Charge Engine," SAE technical paper 820043, 1982.
39. Witze, P.O. "Velocity Measurements in the End-Gas Region During Homogeneous Charge Combustuion in a Spark Ignition Engine," in *Sixth International Symposium on Applications of Laser Techniques to Fluid Mechanics*. Lisbon, 1992.
40. Witze, P.O. and Mendes-Lopes, J.M.C. "Direct Measurement of the Turbulent Burning Velocity in a Homogeneous-Charge Engine," SAE technical paper 861531, 1986.
41. Green, R.M. and Cloutman, L.D. "Planar LIF Observations of Unburned Fuel Escaping the Upper Ring-Land Crevice in an SI Engine," SAE technical paper 970823, 1997.
42. Miles, P.C. and Hinze, P.C. "Characterization of the Mixing of Fresh Charge with Combustion Residuals Using Laser Raman Scattering with Broadband Detection," SAE technical paper 981428, 1998.
43. Miles, P. and Dilligan, M. "Quantitative In-Cylinder Fluid Composition Measurements Using Broadband Spontaneous Raman Scattering," SAE technical paper 960828, 1996.
44. Steinberger, R.L., Marden, W.W., and Bracco, F.V. "A Pulsed-Illumination, Closed-Circuit Television System for Real-Time Viewing of Engine Combustion and Observed Cyclic Variations," SAE technical paper 790093, 1979.
45. Felton, P.G., Mantzaras, J., *et al.* "2-D Visualization of Liquid Fuel injection in an Internal Combustion Engine," SAE technical paper 872074, 1987.
46. Ghandhi, J.B., Felton, P.G., *et al.* "Investigation of the Fuel Distribution in a Two-Stroke Engine with an Air-Assisted Injector," SAE technical paper 940394, 1994.
47. Bardsley, M.E.A., Gajdeczko, B., *et al.* "Measurements of the Three Components of the velocity in the Intake Ports of an I. C. Engine," SAE technical paper 890792, 1989.
48. Bardslev, M.E.A., Felton, P.G., and Bracco, F.V. "2-D Visualization of a Hollow-Cone Spray in a Cup-in-Head, Ported, I.C. Engine," SAE technical paper 890315, 1989.
49. Bardsley, M.E.A., Felton, P.G., and Bracco, F.V. "2-D Visualization of liquid and Vapor Fuel in an I.C. Engine," SAE technical paper 880521, 1988.
50. Ghandhi, J.B. and Bracco, F.V. "Fuel Distribution Effects on the Combustion of a Direct-injection Stratified-Charge Engine," SAE technical paper 950460, 1995.
51. Ghandhi, J.B. and Bracco, F.V. "Mixture Preparation Effects on Ignition and Combustion in a Direct-Injection Spark-Ignition Engine," SAE technical paper 962013, 1996.
52. Fraser, R.A. and Bracco, F.V. "Cycle-Resolved LDV Integral Length Scale Measurements In an I.C. Engine," SAE technical paper 880381, 1988.
53. Fraser, R.A. and Bracco, F.V. "Cycle-Resolved LDV Integral Length Scale Measurements Investigating Clearance Height Scaling, Isotropy, and Homogeneity in an I.C. Engine," SAE technical paper 890615, 1989.
54. Liou, T.-M. and Santavicca, D.A., *Cycle Resolved LDV Measurements in a Motored IC Engine.* J. Fluids Engineering **107**: pp. 232-240, 1985.
55. Hall, M.J. and Bracco, F.V. "A Study of Velocities and Turbulence Intensities Measured in Firing and Motored Engines," SAE technical paper 870453, 1987.
56. Liou, T.M., Hall, M., *et al.* "Laser Doppler Velocimetry Measurements in Valved and Ported Engines," SAE technical paper 840375, 1984.
57. zur Loye, A.O. and Bracco, F.V. "Two-Dimensional Visualization of Premixed-Charge Flame Structure in an IC Engine - SP-715," SAE technical paper 870454, 1987.
58. Mantzaras, J., Felton, P.G., and Bracco, F.V. "Three-Dimensional Visualization of Premixed-Charge Engine Flames: Islands of Reactants and Products; Fractal Dimensions; and Homogeneity," SAE technical paper 881635, 1988.
59. Iijima, T. and Bracco, F.V. "LDV Measurements in an Engine with Square and Circular Piston Cups," SAE technical paper 872073, 1987.
60. Green, R.M. and Cousyn, B.J. "An Optical Research Engine for the Study of Two-Stroke Cycle In-Cylinder Phenomena," pp. 347-352 in *COMODIA 90 - Second Int'l. Symp. on Diagnostics and Modeling of Combustion in IC Engines*, JSME, 1990.
61. Bopp, S.C., Cousyn, B.J., *et al.* "Experimental Study of the Scavenging and Combustion Processes in a Two-Stroke Cycle Research Engine," SAE technical paper 920183, 1992.
62. Miles, P.C., Green, R.M., and Witze, P.O. "In-Cylinder Gas Velocity Measurements Comparing Crankcase and Blower Scavenging in a Fired Two-Stroke Cycle Engine," SAE technical paper 940401, 1994.
63. Konig, G. and Sheppard, C.G.W. "End Gas Autoignition and Knock in a Spark Ignition Engine," SAE technical paper 902135, 1990.
64. König, G., Maly, R.R., *et al.* "Role of Exothermic Centres on Knock Initiation and Knock Damage," SAE technical paper 902136, 1990.
65. Steeper, R.R. and Stevens, E.J. "Characterization of Combustion, Piston Temperatures, Fuel Sprays, and Fuel-Air Mixing in a DISI Optical Engine," SAE technical paper 2000-01-2900, 2000.
66. Bates, S.C. "A Transparent Engine for Flow and Combustion Visualization Studies," SAE technical paper 880520, 1988.

67. Ekchian, A. and Hoult, D.P. "Flow Visualization Study of the Intake Process of an Internal Combustion Engine," SAE technical paper 790095, 1979.
68. Tabaczynski, R.J., Hoult, D.J., and Keck, J.C., *High Reynolds Number Flow in a Moving Corner.* Journal of Fluid Mechanics **42** (2): pp. 249-255, 1970.
69. Maly, R.R., Eberspach, G., and Pfister, W. "Laser Diagnostics for Single-Cycle Analysis of Crank Angle Resolved Length and Time Scales in Engine Combustion," pp. 399-404 in *COMODIA 90 - Second Int'l. Symp. on Diagnostics and Modeling of Combustion in IC Engines*, JSME, 1990.
70. Ziegler, G.F.W., Meinhardt, P.*, et al.* "Cycle-resolved Flame Structure Analysis of Turbulent Premixed Engine Flames," SAE technical paper 905001, 1990.
71. Lawrenz, W., Köhler, J.*, et al.* "Quantitative 2D LIF Measurements of Air/Fuel Ratios During the Intake Stroke in a Transparent SI Engine," SAE technical paper 922320, 1992.
72. Stolz, W., Köhler, J.*, et al.* "Cycle Resolved Flow Field Measurements Using a PIV Movie Technique in a SI Engine," SAE technical paper 922354, 1992.
73. Bräumer, A., Sick, V.*, et al.* "Quantitative Two-Dimensional Measurements of Nitric Oxide and Temperature Distributions in a Transparent Square Piston SI Engine," SAE technical paper 952462, 1995.
74. Borée, J., Maurel, S., and Bazile, R., *Disruption of a compressed vortex.* Phys. Fluids ( Prof. J. Lumley 70th birthday Symp. Papers) **14** (7): pp. 2543-2556, 2002.
75. Marc, D., Boree, J.*, et al.* "Tumbling Vortex Flow in a Model Square Piston Compression Machine: PIV and LDV Measurements," SAE technical paper 972834, 1997.
76. Moreau, J., Boree, J.*, et al.*, *Destabilisation of a compressed vortex by a round jet.* Experiments in fluids **37** (6): pp. 856-871, 2004.
77. Arcoumanis, C., Bicen, A.F., and Whitelaw, J.H., *Measurements in a Motored Four-Stroke Reciprocating Model Engine.* Journal of Fluids Engineering **104** (2): pp. 235-241, 1982.
78. Arcoumanis, C., Bicen, A.F., and Whitelaw, J.H. "Effect of Inlet Parameters on the Flow Characteristics in a Four-Stroke Model Engine," SAE technical paper 820750, 1982.
79. Richman, R.M. and Reynolds, W.C. "The Development of a Transparent Cylinder Engine for Piston Engine Fluid Mechanics Research," SAE technical paper 840379, 1984.
80. Marko, K.A., Li, P.*, et al.* "Flow Field Imaging for Quantitative Cycle Resolved Velocity Measurements in a Model Engine," SAE technical paper 860022, 1986.
81. Regan, C.A., Chun, K.S., and Schock, H.J. "Engine Flow Visualization using a Copper Vapor Laser," pp. 17-27 in *SPIE Vol. 737, New developments and Applications in Gas Lasers*, 1987.
82. Reuss, D.L. "Cyclic Variability of Large-Scale Turbulent Structures in Directed and Undirected IC Engine Flows," SAE technical paper 2000-01-0246, 2000.
83. Reuss, D.L., *Personal communication*, 2014.
84. Reuss, D.L., Kuo, T.-W.*, et al.* "Particle Image Velocimetry Measurements in a High-Swirl Engine Used for Evaluation of Computational Fluid Dynamics Calculations," SAE technical paper 952381, 1995.
85. Kuo, T.-W. and Reuss, D.L. "Multidimensional Port and Cylinder Flow Calculations for the Transparent Combustion Chamber Engine," in *ICE-Vol. 23, Engine Modeling*, ASME, 1995.
86. Le Coz, J.-F., Henriot, S., and Pinchon, P. "An Experimental and Computational Analysis of the Flow Field in a Four-Valve Spark Ignition Engine-Focus on Cycle-Resolved Turbulence," SAE technical paper 900056, 1990.
87. Espey, C. and Dec, J.E. "Diesel Engine Combustion Studies in a Newly Designed Optical-Access Engine Using High-Speed Visualization and 2-D Laser Imaging," SAE technical paper 930971, 1993.
88. Sunnarborg, D.A., "Quick Release Engine Cylinder," in US Patent App., 6158406, 2000.
89. Allen, J., Simms, A.*, et al.* "An Advanced Optically Accessed Single Cylinder Research and Development Engine for Fuel/Air Mixing and Combustion Diagnostics," pp. 595-600 in *Proceedings of the 15th Internal Combustion Engine Symposium (International), No. 9936102*, 1999.
90. Fuyuto, T., Matsumoto, T.*, et al.*, *A New Generation of Optically Accessible Single-Cylinder Engines for High-speed and High-load Combustion Analysis.* SAE Int. J. Fuels Lubr. **5** (1): pp. 307-315, 2011.
91. Müller, S.H.R., Böhm, B.*, et al.*, *Flow field measurements in an optically accessible, direct-injection spray-guided internal combustion engine using high-speed PIV.* Experiments in fluids **48** (2): pp. 281-290, 2010.
92. Calendini, P.O., Duverger, T.*, et al.* "In-Cylinder Velocity Measurements with Stereoscopic Particle Image Velocimetry in a SI engine," SAE technical paper 2000-01-1798, 2000.
93. Nordgren, H., Hildingsson, L.*, et al.* "Comparison Between In-Cylinder PIV Measurements, CFD Simulations and Steady-Flow Impulse Torque Swirl Meter Measurements," SAE technical paper 2003-01-3147, 2003.
94. Glover, A.R., Hundleby, G.E., and Hadded, O. "An Investigation into Turbulence in Engines using Scanning LDA," SAE technical paper 880379, 1988.
95. Foucher, F., Burnel, S., and Mounaïm-Rousselle, C. "Local Flame Front Structure in the Vicinity of the Piston in a Transparent SI Engine," SAE technical paper 2001-01-1957, 2001.

96. Voisine, M., Thomas, L., *et al.*, *Spatio-temporal structure and cycle to cycle variations of an in-cylinder tumbling flow.* Exp. in Fluids **50**: pp. 1393-1407, 2011.
97. Dannemann, J., Pielhop, K., *et al.*, *Cycle resolved multi-planar flow measurements in a four valve combustion engine.* Exp. in Fluids **50, 4**: pp. 961-976, 2010.
98. Mederer, T., Wensing, M., and Leipertz, A. "Investigation of the Interaction of Charge Motion and Residual Gas Concentration in an Optically Accessible SI Engine," SAE technical paper 2013-01-0558, 2013.
99. Dimplefeld, P.M. and Witze, P.O. "Velocity Measurements in a 5.8 Liter Stratified-Charge Rotary Engine," pp. 13.1 in *Fourth International Symposium on Applications of Laser Techniques to Fluid Mechanics*. Lisbon, 1988.